Friction and relative energy dissipation in sheared granular materials

Wan-Jing Wang, Xiang-Zhao Kong,* and Zhen-Gang Zhu†
Key Laboratory of Materials Physics, Institute of Solid State Physics, Chinese Academy of Sciences, P. O. Box 1129, Hefei, Anhui 230031, People's Republic of China
(Received 6 September 2006; published 24 April 2007)

The oscillating cylinder of a low-frequency inverted torsion pendulum is immersed into layers of noncohesive granular materials, including fine sand and glass beads. The relative energy dissipation and relative modulus of the granular system versus the amplitude and immersed depth of the oscillating cylinder are measured. A rheological model based on a mesoscopic picture is presented. The experimental results and rheological model indicate that small slides in the inhomogeneous force chains are responsible for the energy dissipation of the system, and the friction of the grains plays two different roles in the mechanical response of sheared granular material: damping the energy and enhancing the elasticity.

DOI: 10.1103/PhysRevE.75.041302 PACS number(s): 45.70.−n, 62.20.Dc, 62.40.+i, 81.05.Rm

I. INTRODUCTION

Granular materials are composed of many solid particles interacting solely via the contact force. The mechanical response of a granular medium to shear force is a fundamental property of these materials and is very important to any industrial process [1–3]. The literature presented indicates that under different sheared boundaries the granular medium shows different mechanical properties. If a large object moves slowly in a medium, one can observe a fluctuating force distribution resisting the motion, showing stick-slip characteristics [4,5]. But, during the quasistatic interval, the object is at rest and the granular material can sustain the exerted shear stress [3]. Here, we will focus on the quasistatic regime, in which a weak shear stress is supposed to slightly deform the granular medium without actually modifying the static configuration.

Due to gravity, "granular gases" rapidly organize into a static assembly as "granular solids." This also is a process of energy dissipation, as granular solids rapidly damp energy released by shocks of external forcing. Due to the complex disordered structure and highly nonlinear internal friction [4], the energy dissipation in dense granular materials is a much more difficult problem, and many phenomena in granular solids are still not fully understood and required further investigation.

In Ref. [5], D'Anna investigated the quasistatic mechanical properties of a sheared granular medium by a low-frequency torsion pendulum. The loss factor as a function of torque is studied and a simple rheological model is presented. Then the position of the peak in the loss factor has been used to measured the static friction coefficient in granular systems. However, fitting the data to the model is only relatively satisfying. In particular, the sharp onset of the peak predicted by the model is observed only when the probe surface is clean.

In this paper we will investigate the dissipation in a quasistatic granular system further. The oscillating member of an inverted torsion pendulum is immersed into the granular material, as shown in Fig. 1, and the response to a harmonic torque is measured. Some additional results are obtained, e.g., with increase of the immersed depth a drop in the relative energy dissipation (RED) is observed. In addition, some smoother profiles are demonstrated, because the inverted torsion pendulum can prevent sideways movement rather better.

Our model is also built on D'Anna's model [5]. In Sec. IV A we changed the variable of the model and found it is invalid in explanation of our experimental results. Then we present our model based on the mesoscopic picture in Sec. IV B. This model of a series of slipping units gives more details of the energy dissipation. It not only indicates the presence of the peak of the dissipation, but also explains the dissipative mechanism before the peak. Then the paper discusses the two roles of friction in granular media. The me-

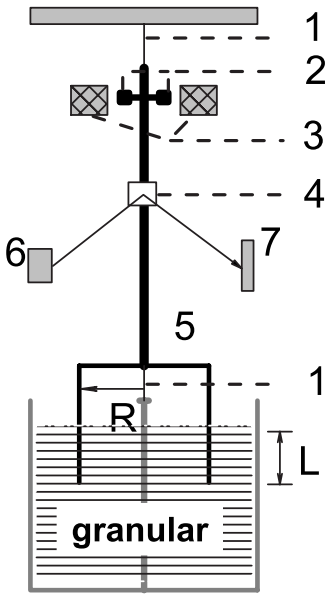

FIG. 1. Sketch of the forced torsion pendulum immersed into a granular medium. 1, suspension wires; 2, permanent magnet; 3, external coils; 4, mirror; 5, cylinder (made of aluminum alloy with inner radius R) covered or not by a fixed layer of granules; 6, optic source; 7, optic detector.

*Present address: Environmental Engineering, ETH-Zurich, Zurich, CH-8093, Switzerland.
†Electronic address: zgzhu@issp.ac.cn

soscopic model shows clearly that friction can enhance the elasticity of a granular system.

II. EXPERIMENT

The inverted torsion pendulum (see Fig. 1) consists of a cylinder that is able to rotate around its axis, but prevented from moving sideways by two suspension wires fixed to the two ends of the cylinder. The cylinder is forced into torsional vibration by a time-dependent force $F(t)=F_0\sin(\omega t)$, exerted by applying a pair of permanent magnets fixed to the pendulum and external coils (circulating an ac current). The angular displacement function of the cylinder, $A(t)$, is measured optically. In the case here, the response of the argument $A(t)=A_0\sin(\omega t+\delta\alpha)$, where $\delta\alpha$ is the phasic difference between $A(t)$ and $F(t)$. The damping properties of an oscillating system are characterized by the RED η, the ratio of damping energy per oscillating cycle of the applied force, i.e., $\eta=Q/2\pi W$, where Q is the damping energy per cycle, and W is the maximum stored energy per cycle. For a linear system [6], the RED is given by $\eta\equiv\tan(\delta\alpha)$. In a nonlinear system as in the case here [5], the RED is given by its first approximation as $\eta\simeq\tan(\delta\alpha)$.

In our experiments, the cylinder (with inner radius $R=17$ mm and a 1-mm-thick wall) is immersed into a large assembly of granules held in a large enough container (with inner radius $R_0=38$ mm). The experiments are conducted in granular systems respectively composed of glass beads and fine sand, with the same diameter of $d=0.054-0.11$ mm. Note that the glass beads are spherical with a smooth surface, and fine sand is natural sand with a rough surface. Two situations are considered here: the immersed cylinder is clean, and the immersed cylinder is covered by a layer of grains glued on with epoxy. In order to eliminate the effect of the construction history, the cylinder is pushed to a certain depth in the granular assembly. Before each experiment, the granular system is flattened and vibrated by external vibrations to ensure the accuracy of the measurements. Our experiments are performed at uncontrolled ambient humidity, and the whole system is placed on an antivibrational table to prevent undesired vibration-induced effects. In our experiments the maximum angular displacement is below 0.4° ($\pi R0.4/180<0.1d$, where the real displacement of the cylinder is less than $0.1d$, relative to the particle size). The frequency of 0.6 Hz, which is well below the inherent frequency of the pendulum (about 36 Hz), is chosen as the forced frequency of the pendulum here. The RED of the suspension wires is of the order of about 10^{-3}, and can be assumed to be elastic.

III. RESULTS

In the measurements of the RED and the relative modulus, given by $\eta=\tan(\delta\alpha)$ and $G_0=F_0/A_0$, respectively, as functions of the amplitude A_0 and the immersed depth L/d, we systematically observe the dissipation properties of granular system under small torsion amplitudes.

Figures 2 and 3 show the RED obtained in a fine sand system, while Figs. 4 and 5 show the RED obtained in a glass bead system, with a cylinder covered by a layer of glued grains and a clean cylinder, respectively (see the caption of each figure). The following characteristics can be easily picked out from these figures of the RED for different granular systems.

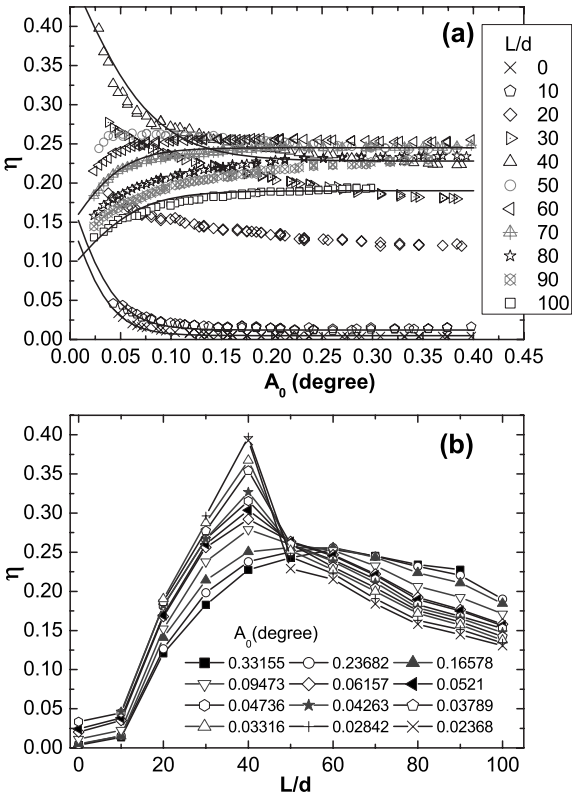

FIG. 2. RED of a fine sand assembly, with the oscillating cylinder covered by a layer of grains. (a) η vs A_0 for different immersed depths, as noted. The solid lines are fitted by $\eta=a\tanh(bA_0)+c$, where a, b, and c are fitting parameters. Here only five lines are presented. (b) η vs L for different oscillating amplitudes A_0, as noted.

(1) Figures 2(a), 3(a), 4(a), and 5(a) show the profiles of RED versus the torsional amplitudes A_0. Except for a transition interval of immersed depth L, the RED η can be well fitted by $\eta=a\tanh(bA_0+c)$ [see Figs. 2(a) and 3(a)], where a,b, and c are fitting parameters clearly dependent on L. The parameter a shows a transition from $a<0$ to $a>0$ as L increases. When the immersed depth L is small, η deceases monotonically with increasing amplitude A_0, corresponding to $a<0$. After the transition interval, η increases monotonically with A_0, corresponding to $a>0$. Within the transition interval, η shows a peak.

(2) As shown in the profiles of η vs L/d [see Figs. 2(b), 3(b), 4(b), and 5(b)], η increases with increasing immersed depth L for a given amplitude A_0 until it approaches the maximum η^* at a critical depth L_c. After that, η decreases with increasing immersed depth. One might consider that the more grains are vibrated, the less energy is dissipated. This is not understood.

(3) With decreasing amplitude A_0, L_c shifts from large small values of L, and stops at $L/d\simeq 30$ for different situations in our experiments. The value of η^* decreases with increasing $L_c(A_0)$.

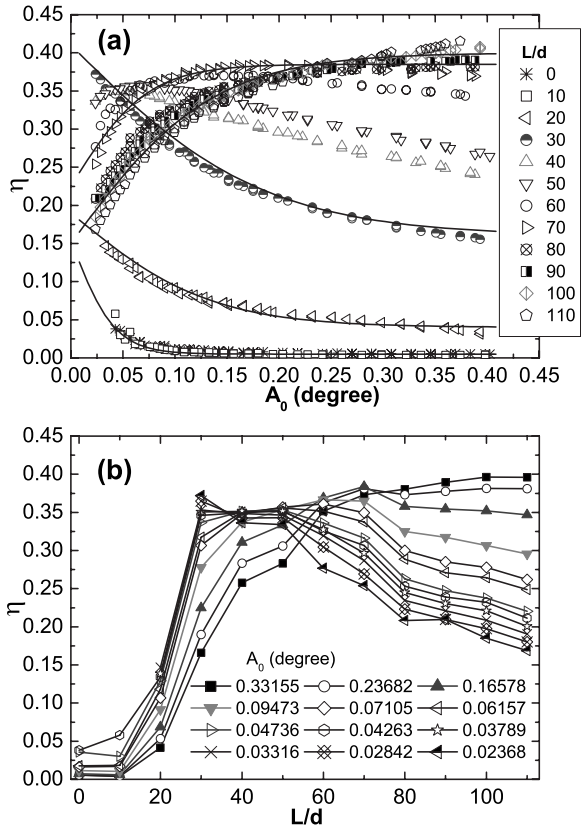

FIG. 3. RED of a fine sand assembly, with a clean oscillating cylinder. (a) η vs A_0 for different immersed depths, as noted. The solid lines are fitted by $\eta=a\tanh(bA_0)+c$. Here only five lines are presented. (b) η vs L for different oscillating amplitudes A_0, as noted.

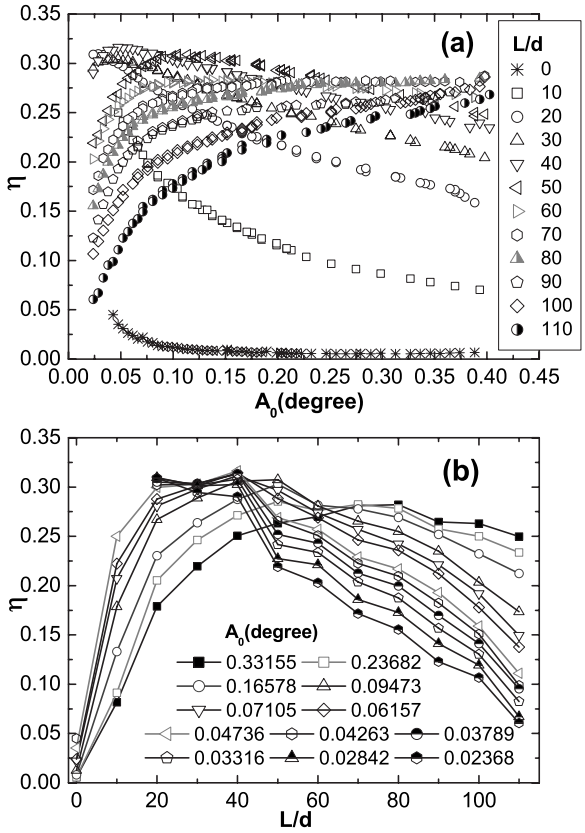

FIG. 4. RED of an assembly of glass beads, with the oscillating cylinder covered by a layer of grains. (a) η vs A_0 for different immersed depths, as noted. (b) η vs L for different oscillating amplitudes A_0, as noted.

(4) In the profiles of η vs L/d, after the peak of η the decrease of η is 0.03–0.26 for the fine sand system and 0.05–0.25 for the glass bead system with the covered cylinder, while with the clean cylinder the decrease of η is 0.0–0.20 and 0.0–0.17, respectively. There is little difference in the range of decrease of η between the two situations of a covered and a clean cylinder. However, the rate of decrease of η is apparently different between the two situations. As shown in the profiles of η vs A_0, with increasing L, after the transition interval, the curves of η are very close to each other for the clean cylinder, while the curves are more discrete in the same interval for the covered cylinder.

(5) With the same cylinder (clean or covered), the rate of decrease of η is also different between the two granular systems. In particular, just over the peak of η^*, the decrease of η in the fine sand system is larger than that of the glass bead system [compare Figs. 2(b) and 4(b), 3(b) and 5(b)]. This difference gets more obvious at low amplitude, and η of the fine sand system drops by more than 0.16 just over η^* with the amplitude $A_0=0.023\,68°$ and an increment of $L=10d$ [see Fig. 2(b)].

Figure 6 shows the relative modulus obtained in a fine sand system using a cylinder covered by a layer of glued grains. As the data show in Fig. 6(a), the relative modulus G_0 decreases with increase of the torsion amplitude at a given depth. After rearranged treatment of the data, we get the profiles of the relative modulus of G_0 versus L/d, for different torsional amplitude. With increase of the immersed depth, the modulus G_0 increases monotonically. As shown in Fig. 6(b), the relative modulus is an almost linear function of the immersed depth L/d, e.g., $G_0=k_1L/d+k_2$, where k_1 (>0) and k_2 are fitting parameters. The slope k_1 increases with decreasing amplitude. Here we just show the profiles of the relative modulus in a fine sand system with a covered cylinder; however, other situations have similar profiles.

IV. MODELING

A. Rheological model

In Ref. [5], a simple rheological model, as shown in Fig. 7(a), is presented to reproduce the RED measured in granular materials. In the model, the spring G_p represents the suspension wires of the pendulum, which is a perfectly elastic unit. Another branch represents the granular medium, characterized by a slide unit with a critical torque T_c and a spring of torsion constant G_g. The slide unit and the spring G_g are series wound. The response of the lower branch is nonlinear and is given by $T=G_gA$ for $A<A_c$ and $T=G_gA_c$ for $A>A_c$, where $A_c=T_c/G_g$, is the critical amplitude for the slide unit beginning to slide.

The RED is the relative dissipation of energy per torsional cycle, given by $\eta=Q/2\pi W$, where Q is defined as the dissi-

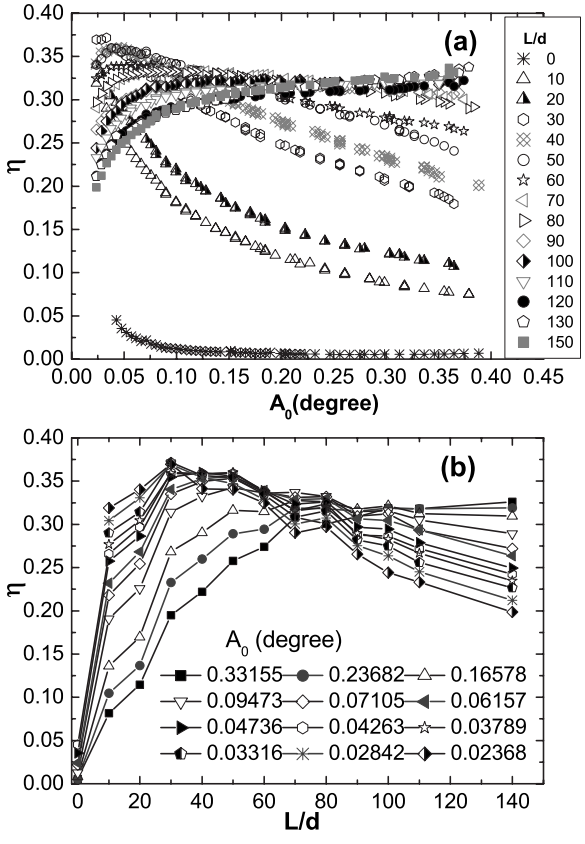

FIG. 5. RED of an assembly of glass beads, with the clean oscillating cylinder. (a) η vs A_0 for different immersed depths, as noted. (b) η vs L for different oscillating amplitudes A_0, as noted.

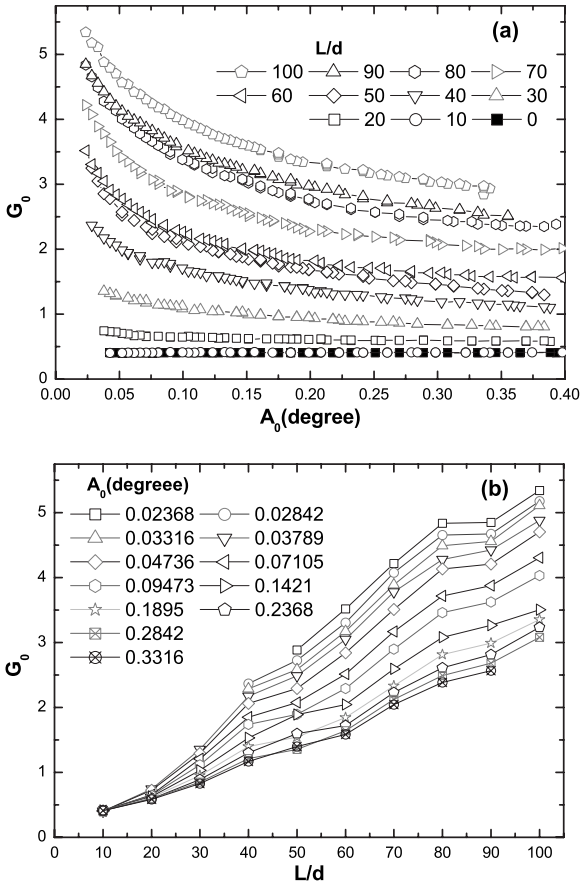

FIG. 6. Relative modulus of a fine sand assembly, with the oscillating cylinder covered by a layer of grains. (a) G_0 vs A_0 for different immersed depth, as noted. (b) G_0 vs L/d for different oscillating amplitude A_0, as noted.

pated energy of the slide unit and W is the elastic energy stored in the two springs during loading. Under harmonic torsional shear, Q and W can be written as

$$Q = 4T_c(A_0 - A_c), \tag{1}$$

$$W = G_p(A_0)^2/2 + G_g(A_c)^2/2. \tag{2}$$

Adopting the notation $\chi = G_g/G_p$, the RED η is easily obtained:

$$\eta = \frac{4}{\pi}\frac{\frac{A_0}{A_c} - 1}{\frac{1}{\chi}\left(\frac{A_0}{A_c}\right)^2 + 1} \tag{3}$$

for $A_0/A_c > 1$ and $\eta = 0$ for $A_0/A_c < 1$. The RED is shown in Fig. 7(b) as a function of A_0/A_c with different χ.

The modulus of the system is defined as $G = T/A$ and is written

$$G = G_p\left(1 + \frac{\chi}{A_0/A_c}\right) \tag{4}$$

for $A_0/A_c > 1$, and $G = G_p + G_g$ for $A_0/A_c < 1$. The normalized modulus G/G_p is shown in Fig. 7(c) as a function of A_0/A_c for different χ.

This rheological model provides a basic, macroscopic understanding of the observed mechanical behavior. Due to gravity, grains organize into a static assembly and the pressure in the granular material increases linearly with increase of the depth from the surface [7]. In the continuum approach [8], the pressure P at a given depth l is written $P = K\rho g l$, where K is a constant that characterizes the pressure anisotropy, ρ is the granular density, and g is the acceleration of gravity. Based on the definition of the RED we know that the dissipation of energy results from the frictional sliding of the slide unit. In this approach, the critical torque, over which the sliding begins, can be seen as the macroscopic failure limit, i.e., $T_c = T_f$. It is given by [5]

$$F_f = 2\mu_s K\pi\rho g L^2 R, \tag{5}$$

where μ_s is the coefficient of static friction, L is the immersed depth, and R is the cylindrical radius. With increasing immersed depth, grains in the deeper layer will provide a larger recovery force, and the granular modulus G_g will rise, which means that $\chi = G_g/G_p$ increases with the immersed depth L. (The detailed explanation will be given in the next section.)

Now we take a look at the comparison between the experimental data and the results of the rheological model. In the model, we just consider the RED for $A_0/A_c > 2$ [see Fig. 7(b)], corresponding to the beginning amplitude of this ex-

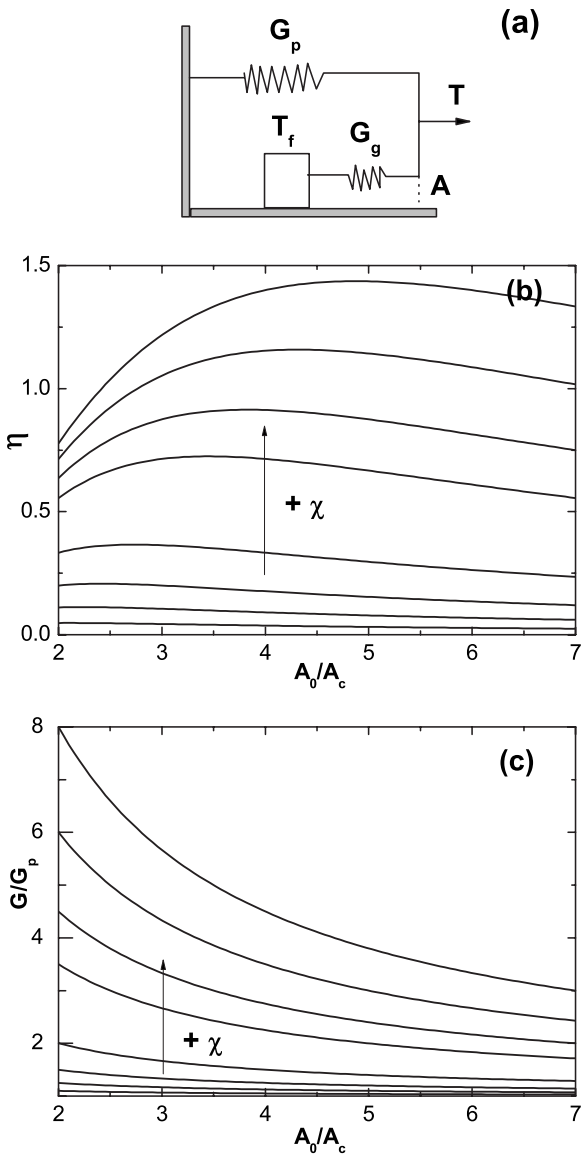

FIG. 7. (a) Rheological model. The lower branch represents the granular medium, characterized by a slide unit of critical torque T_c and a spring of torsion constant G_g. The upper branch represents the suspension wires of the pendulum, of torsion constant G_p. (b) The RED $\eta=Q/2\pi W$ and (c) the modulus G calculated from the rheological model, potted as a function of the normalized amplitude A_0/A_c for different χ. The various curves correspond to an increasing χ of 0.2, 0.5, 1, 2, 5, 7, 10, and 14, respectively.

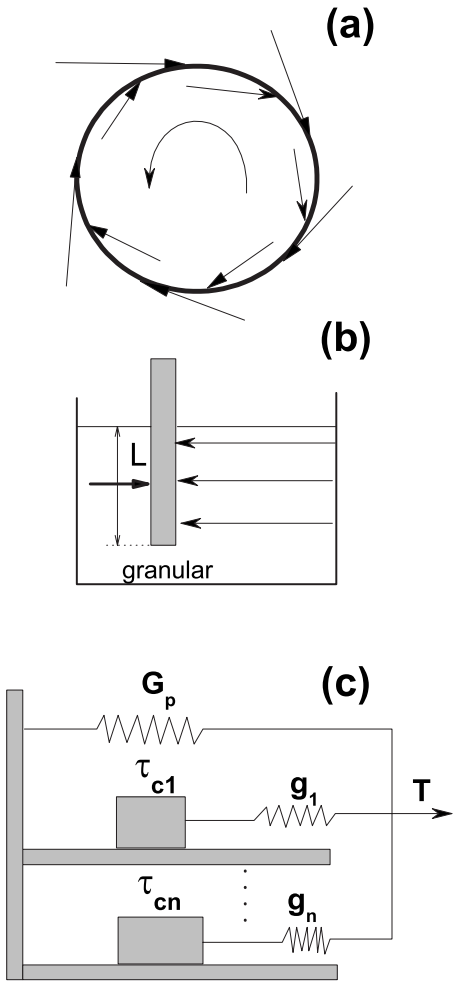

FIG. 8. Schematic distribution of force chains opposing (a) the rotation of the pendulum and (b) the straight motion of an immersed object, where L is the immersion depth. (c) The mesoscopic rheological model.

periment, 0.023 68°. For $2<A_0/A_c<7$, the results of the rheological model are relatively satisfactory in fitting the experimental data. The RED also decreases monotonically with increasing A_0/A_c when χ is small. With increasing χ, the maximum of η shifts into this section. This can be considered as a transitional interval, as shown in experiments. After the interval, η increases monotonically with A_0/A_c. The modulus G calculated from the rheological model, as a function of A_0/A_c with different χ, is similar to the data from experiment [see Figs. 6(a) and 7(c)]. However, a difference about η between the rheological model and experiments is that η increases monotonically with increasing χ (and L) in the simple rheological model, while in the experiment η drops with increasing immersed depth over the critical depth L_c. The model cannot explain all the experimental results. In the following section we will try to give a mesoscopic explanation and show the two roles of friction in the damping of energy.

B. Mesoscopic picture

Noting that the granular material is a relatively discrete medium and the distribution of force is inhomogeneous on the granular length scale, we need to take into account explicitly the complexity of force transmission in the medium, and the force distribution opposing the rotation of the pendulum at a given moment during the oscillating cycle. Considering a cylindrical probe rotating in a granular medium, the spatial force distribution around the probe is likely to be organized along directions almost tangential to the cylinder, where the maximum stress can build up many chains of grains, as sketched in Fig. 8(a). During rotation, the compressive stress supported by chains of grains aligned along quasitangential trajectories plays a more significant role than

the compressive stress oriented in radial directions. (For a hollow cylinder, the force chain on the inside of the cylinder will be different from that on the outside of the cylinder. However, the diameter of the cylinder in our experiments is rather large compared to the diameter of the particles and the length of the force chain. Here we do not consider these differences.) In the vertical direction the torque resisting the rotation has a similar origin to the drag force opposing the straight motion of an immersed object [Fig. 8(b)], i.e., the random buckling of the force chain in front of the object, where compressive stress is continuously built up and released [5].

We divide the system into $n=L/d_g$ discrete horizontal layers of thickness d_g. Under small torsional strain, the discrete horizontal layers can be considered as an elastic solid [9]. When the immersed cylindrical probe rotates in the granular medium, these discrete horizontal layers provide a series of drag torques τ_i, where $i=1,2,\ldots,n$. A drag torque is provided by many chains of grains in the layer. These force chains, which originate from the surface of the immersed cylinder and extend a few grain diameters [1,2,10] actually bifurcate and follow nonlinear paths. The force chains of a layer are stable, until the local force between a pair of grains somewhere in the layer is larger than the critical friction force f_c, above which this pair of grains slip relative to each other. (The distance of the slide is smaller than a grain diameter and this slide cannot induce a rearrangement of force chains. It can be considered as a relative slide between asperities at the surfaces of grains [3,5,11].) The maximum loading shear strain of a layer is given by $A_{ci}=f_c/g_i$, where g_i is the elastic modulus provided by the force chains within one layer of grains. The elastic modulus g_i is related to the restitution coefficient of granular material, which is assumed to be a constant. So here g_i is considered as a constant for a finite torsional amplitude. The critical friction force f_c can be approximately given by$f_c=\mu_s K\rho g l$, where μ_s is the coefficient of static friction. We easily obtain

$$A_{ci} \propto \mu_s \rho l_i, \tag{6}$$

where l_i is the depth of the ith layer.

Based on the above mesoscopic picture, we present a mesoscopic rheological model. In the simple model there is only one nonlinear branch representing the whole granular system, while here we assume there is a series of branches [see Fig. 8(c)] corresponding to the different horizontal layers at different immersed depths.

From Eq. (6), we know that, with a given immersed depth and a given torsional amplitude, e.g., $A_0=0.023\,68°$, a number of horizontal layers will present relative sliding. When the immersed depth is rather small, all layers will join in the slides for $A_0=0.023\,68° > A_{cn}$ corresponding to the situation that the immersed depth is smaller than $30d$ in experiments. With increasing immersed depth, layers below this critical depth ($30d$ corresponding to $A_0=0.023\,68°$) will not join in slides. Under torsional shear, these layers just show elasticity. In this condition, all layers can be simply divided into two branches: the higher branch, which presents slides and joins in damping, and can be approximately characterized by a summed modulus G_a and a summed critical friction T_a; and the lower branch, which only provides elasticity, and can be approximately characterized by a summed elastic modulus G_b.

Defining the notation $A_c=T_a/G_a$ in this mesoscopic model, we obtain the RED

$$\eta = \frac{4}{\pi} \frac{\dfrac{A_0}{A_c} - 1}{\dfrac{G_p + G_b}{G_a}\left(\dfrac{A_0}{A_c}\right)^2 + 1} \tag{7}$$

for $A_0/A_c > 1$, and $\eta=0$ for $A_0/A_c < 1$. The modulus can be similarly written as

$$G = G_p + G_b + \frac{G_a}{\dfrac{A_0}{A_c}} \tag{8}$$

for $A_0/A_c > 1$, and $G=G_p+G_b+G_a$ for $A_0/A_c < 1$.

With a given torsional amplitude A_0, there is a corresponding critical depth L_c, which is the depth of the layers presenting slides and ranking as the upper branch. Let the thickness of a layer $d_g=10d$; then $G_a=n_0 g_i$ and $G_b=(n-n_0)g_i$, where $n_0=L_c/d_g$ and $n=L/d_g$. The notation $\chi=(G_a+G_b)/G_p$ can be written

$$\chi = \frac{n}{k}, \tag{9}$$

where $k=G_p/g_i$.

Note that $G_b=0$, when $n/n_0<1$. So we obtain the RED as a function of the amplitude A_0/A_c and immersed depth $n=L/10d$,

$$\eta = \frac{4}{\pi} \frac{\dfrac{A_0}{A_c} - 1}{\dfrac{k}{n}\left(\dfrac{A_0}{A_c}\right)^2 + 1} \tag{10a}$$

for $n < n_0$;

$$\eta = \frac{4}{\pi} \frac{\dfrac{A_0}{A_c} - 1}{\left(\dfrac{k}{n_0} + \dfrac{n}{n_0} - 1\right)\left(\dfrac{A_0}{A_c}\right)^2 + 1} \tag{10b}$$

for $n > n_0$. As shown in Fig. 9, we obtain two profiles of η as indicated in the caption of the figure.

Similarly, the modulus can be written

$$G = G_p\left(1 + \frac{\dfrac{n}{k}}{\dfrac{A_0}{A_c}}\right) \tag{11a}$$

for $n < n_0$;

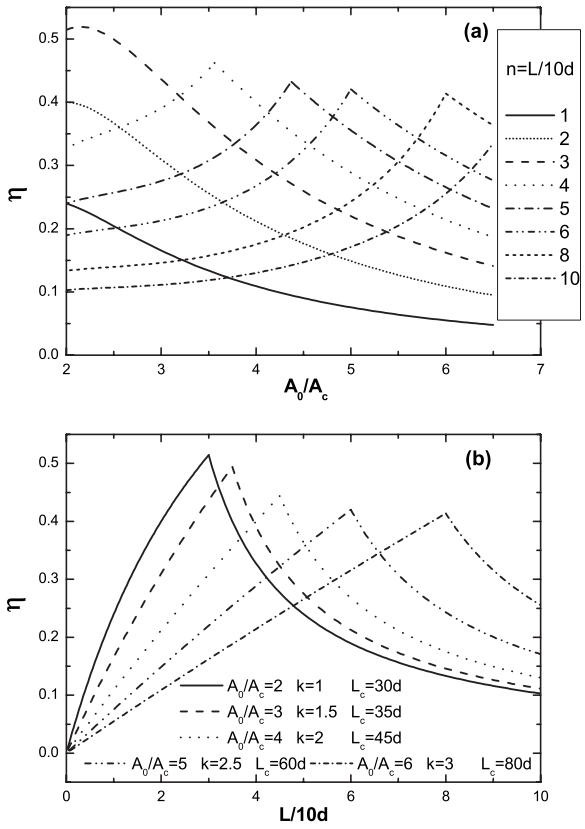

FIG. 9. RED η versus (a) torsion amplitude, for different immersed depths, as noted; and (b) immersed depth $L/10d$, calculated from the rheological model based on the mesoscopic picture, for different torsion amplitudes, as noted.

$$G = G_p\left(1 + \frac{n - n_0}{k} + \frac{n_0/k}{A_0/A_c}\right) \tag{11b}$$

for $n > n_0$. These equations denote that the modulus always is a linear function of the immersed depth, as shown in Fig. 6(b).

V. DISCUSSION AND OPEN QUESTIONS

In Eq. (10), for a small depth, the RED decreases monotonically with increasing A_0/A_c, just as shown in Fig. 9(a) for $n \leq 3$. This dissipation comes from the frictional sliding. In this condition, the RED increases with increasing immersed depth L/d, as shown in Fig. 9(b). When the immersed depth exceeds the critical depth L_c, the layers of grains below the critical depth will only provide elasticity, which will enhance the elasticity of the system. As a result, the RED will decrease with increasing immersed depth, which corresponds to a drop of η vs L/d over the critical depth L_c, as shown in Fig. 9(b). With increasing torsional amplitude, these elastic layers will be reduced and even vanish, so that the position of the peak in the profiles of η vs L shifts to larger L, corresponding to a shift of critical depth. These details of dissipation cannot been given by the simple rheological model.

Equation (6) also denotes that the characteristics of the grains, including μ_s and ρ, play a key role in determining the maximum loaded amplitude (above which sliding occurs) of the discrete grain layers. A simple sliding experiment indicates that the frictional coefficient of the covered cylinder is about twice as much as that of clean cylinder. Therefore, when the loading amplitude exceeds A_c, for a clean cylinder, the sliding will mostly happen at the surface of the cylinder. In contrast, the sliding occurs somewhere in the granular layer for a covered cylinder. This results in a decrease of the critical depth L_c for the clean cylinder, which is in agreement with the results of experiments (see Figs. 2(a) and 3(a)). It also results that, above the peak of η, the decrease and the rate of decrease of η in the case of the covered cylinder are larger than those of the clean probe, whether for fine sand or glass beads, as shown in Figs. 2(b), 3(b), 4(b), and 5(b). Because the friction coefficient and density of fine sand are larger than those of glass beads, the data of our experiments show that the rate of decrease of η vs L/d in fine sand system is larger than that in glass beads for the same cylinder in this range [compare Fig. 2(b) with 4(b), and 3(b) with 5(b)]. This difference becomes more obvious at lower amplitudes.

The analysis indicates that the friction in a granular medium plays two roles in our experiment. The physical definition of η denotes that the friction induces energy dissipation. In the mesoscopic model it also is the basis of the elasticity and can even enhance the elasticity of the system. The results of experiments directly show this phenomenon. The RED in the case of a covered cylinder for the two granular systems is slightly larger than that of a clean cylinder in approaching the peak of η (refer to the profile of η vs L/d), where the dissipation role is obvious; above the peak (for $L > L_c$), the RED in the case of the covered cylinder is apparently less than that of the clean cylinder, where the friction enhances the elasticity of the system. So one can view the critical depth L_c as the transition depth, on the two sides of which the friction of the granular medium plays two different roles.

In Ref. [5], D'Anna presented a simple rheological model to reproduce the data. The simple model assumed that all the discrete layers will exceed the critical friction torque simultaneously. So the model predicted a sharp onset; however, this is observed only when the probe surface is clean. According to our mesoscopic rheological model, the exceeding actually occurs layer by layer with increasing torsional amplitude. So the gradual increase of dissipation before the peak can be understood easily.

The above discussion indicates that the mesoscopic rheological model has provided more information about dissipative properties. However, one also can find that the details of the profiles in the Fig. 9 are not good in fitting to the results of experiments. These inconsistencies in a pictorial sense result from the simplification of the model. In the mesoscopic picture, we know that every branch has a different critical amplitude and thus the energy dissipation is a variable of the torsional amplitude for different horizontal layers. But in the calculation we have simply divided all layers into two branches. Further investigation is needed.

For beads with a diameter smaller than 0.5 mm, humidity has been found to strongly influence the friction coefficient of granular matter, most likely due to the formation of liquid

bridges between grains [12]. These experiments are carried out in realistic ambient humidity. Although dry grains are used, we do not think that adhesive effects can be eliminated in the observations. Hence the questions are whether liquid bridges play a very important role in the laboratory atmosphere and how do the observations change if the humidity is varied, e.g., when wet particles are used.

VI. CONCLUSION

To conclude, this paper systematically elucidated the dissipative mechanism of a granular system under low torsional shear, through measurements of the RED versus the amplitude A_0 and the immersed depth L/d. A rheological model based on the mesoscopic picture is presented to reproduce the experimental results.

This work is focused on the quasistatic, dissipative regimes where the grains stick or slip relative to each other. This transition from stick to slip is determined by the torsional amplitude and the immersed depth of the probe. The rheological model also displays an approximate expression of the RED as a function of the amplitude and the depth. This is an essential question for researchers investigating the stability of buildings, silos, and slopes—particularly for predicting earthquakes and avalanches [13,14].

Experiments also show the two different roles of friction: when the friction is not large enough, it increases energy dissipation and renders the response more anisotropic; when the friction is large enough, it enhances the elasticity of the system and renders the response more isotropic. This can be considered as evidence for the conclusion of Goldenberg and Goldhirsch [9,14] in realistic, large-scale, and three-dimensional granular systems. These general conclusions show the potential of this experiment in understanding the granular mechanical properties at the mesoscopic level.

ACKNOWLEDGMENTS

This work is financially supported by the National Natural Science Foundation of China under Grant No. 10374089 and the Knowledge Innovation Program of the Chinese Academy of Sciences under Grant No. KJCX2-SW-W17.

[1] See, for example, H. Jaeger, S. R. Nagel, and R. P. Behringer, Rev. Mod. Phys. **68**, 1259 (1996); H. M. Jaeger and S. R. Nagel, Science **255**, 1523 (1992); J. M. Carlson, J. S. Langer, and B. E. Shaw, Rev. Mod. Phys. **66**, 657 (1994).

[2] B. Miller, C. O'Hern, and R. P. Behringer, Phys. Rev. Lett. **77**, 3110 (1996).

[3] S. Nasuno, A. Kudrolli, and J. P. Gollub, Phys. Rev. Lett. **79**, 949 (1997).

[4] R. Albert, M. A. Pfeifer, A.-L. Barabasi, and P. Schiffer, Phys. Rev. Lett. **82**, 205 (1999); I. Albert, P. Tegzes, B. Kahng, R. Albert, J. G. Sample, M. Pfeifer, A.-L. Barabasi, T. Vicsek, and P. Schiffer, *ibid.* **84**, 5122 (2000).

[5] G. D'Anna, Phys. Rev. E **62**, 982 (2000).

[6] A. S. Nowick and B. S. Berry, *Anelastic Relaxation in Crystalline Solids* (Academic Press, New York, 1972).

[7] L. Vanel, P. Claudin, J. P. Bouchaud, M. E. Cates, E. Clement, and J. P. Wittmer, Phys. Rev. Lett. **84**, 1439 (2000).

[8] R. M. Nedderman, *Statics and Kinematics of Granular Materials* (Cambridge University Press, Cambridge, U.K., 1992).

[9] C. Goldenberg and I. Goldhirsch, Nature (London) **435**, 188 (2005).

[10] C.-H. Liu *et al.*, Science **269**, 513 (1995).

[11] J. L. Anthony and C. Marone, J. Geophys. Res. **110**, B08409 (2005).

[12] L. Bocquet, E. Charlaix, S. Ciliberto, and J. Crassous, Nature (London) **396**, 735 (1998); R. Brewster, G. S. Grest, J. W. Landry, and A. J. Levine, Phys. Rev. E **72**, 061301 (2005).

[13] A. Daerr and S. Douady, Nature (London) **399**, 241 (1999); G. D'Anna and G. Gremaud, *ibid.* **413**, 407 (2001).

[14] S. Luding, Nature (London) **435**, 159 (2005).